Earthq Eng & Eng Vib (2015) 14: 663-681 **DOI**: 10.1007/s11803-015-0052-z

A stochastic based approach for a new site classification method: application to the Algerian seismic code

Mohamed Beneldjouzi[1†] and Nasser Laouami[2‡]

1. *Civil Engineering Faculty, University of Sciences and Technology Houari Boumediene, Algiers 16111, Algeria*

2. *Earthquake Engineering Applied Research Center* (*CGS*)*, Rue Kaddour Rahim, Algiers, 16040, Algeria*

Abstract: Building codes have widely considered the shear wave velocity to make a reliable subsoil seismic classification, based on the knowledge of the mechanical properties of material deposits down to bedrock. This approach has limitations because geophysical data are often very expensive to obtain. Recently, other alternatives have been proposed based on measurements of background noise and estimation of the H/V amplification curve. However, the use of this technique needs a regulatory framework before it can become a realistic site classification procedure. This paper proposes a new formulation for characterizing design sites in accordance with the Algerian seismic building code (RPA99/ver.2003), through transfer functions, by following a stochastic approach combined to a statistical study. For each soil type, the deterministic calculation of the average transfer function is performed over a wide sample of 1-D soil profiles, where the average shear wave (S-W) velocity, V_s, in soil layers is simulated using random field theory. Average transfer functions are also used to calculate average site factors and normalized acceleration response spectra to highlight the amplification potential of each site type, since frequency content of the transfer function is significantly similar to that of the H/V amplification curve. Comparison is done with the RPA99/ver.2003 and Eurocode8 (EC8) design response spectra, respectively. In the absence of geophysical data, the proposed classification approach together with micro-tremor measures can be used toward a better soil classification.

Keywords: random field; transfer function; soil classification; RPA99/ ver. 2003; EC8; site factor; response spectrum

1 Introduction

Local geological conditions have a strong influence on ground surface motion, and analysis of local site response is fundamental to seismic hazard assessment (Lermo and Chávez-García, 1993; Cadet *et al*., 2008). In particular, layer softless consolidated sedimentary deposits overlaying bedrock could lead to further amplification but information on these deposits is generally hard to obtain due to technical and/or financial constraints. For this reason amplification studies are not commonly performed in new projects and instead sites are routinely classified with respect to soil classes adopted in many seismic building codes. These soil classes are based on the average shear wave (S-W) velocity at the upper 30 meters of the subsurface geological materials, $V_{s,30}$, and the dominant period. Both parameters also affect the normalized elastic response spectra. The main weakness of a $V_{s,30}$ denominated classification is that it cannot quantify properly the effects of the impedance contrast, which is one of the main sources of soil amplification (Pitilakis *et al*., 2004).

A brief review is given in the following. The most elementary technique for site classification is borehole data. However, with the increase in the number of strong ground motion stations many other methods were successful. Most of these methods are based on the determination of the site's predominant period, without providing a reliable assessment of the surface ground motion amplification needed in structural dynamic analysis. The Standard Spectral Ratio (SSR) method was initially put in practice by Borcherdt and Gibbs (1970). It is based on comparing micro-tremors or earthquake signals recorded over a site with unknown conditions and those obtained at a nearby reference rock site. The major inconvenience of this method remains the need of a reference rock station (Lermo and Chavez Garcia, 1993; Seo *et al*., 1996), and in that event alternative empirical techniques could be used. The receiver functions technique was proposed by Langston (1979), where the reference station response can be substituted by the vertical component measured at the same station since it is considered not to be affected by the local amplification. It should also be mentioned that both

Correspondence to: Mohamed Beneldjouzi, Civil Engineering Faculty, University of Sciences and Technology Houari Boumediene (USTHB), BP 32 El Alia, Bab Ezzouar, Alger, 16111, Algeria
Tel: +213 550951306
E-mail: mohamedb_in@yahoo.fr
†Assistant Professor; ‡Associate Professor
Received June 12, 2014; **Accepted** December 26, 2014

receiver functions and SSR methods give only the site's particular information such as the resonance frequency (Riepl *et al*., 1998), although it is a primary parameter in site categorization schemes.

In earlier studies on site effects characterization, the horizontal-to-vertical spectral ratio (HVSR) technique is one of the successfully used methods, firstly introduced by Nogoshi and Igarashi (1971) and enhanced later by Nakamura (1989). This method is based on the H/V ratio of the Fourier spectrum performed on ambient noises and extended to the use of earthquake recordings. In the case of micro-tremor records, it gives an accurate reading of the site's predominant frequency (Nakamura, 1989; Bard, 1999). In 2010, Wen (Wen *et al*., 2010) successfully used HVSR technique for classifying sites of strong motion stations after the Wenchuan earthquake (China) to determine fundamental frequencies of the affected sites. The use of the above techniques demonstrated, however, that they are not able to capture reliable information on a site's amplification.

An empirical site classification method similar to the receiver functions approach, based on the HVSR of earthquake records was proposed by Zhao *et al.* (2004, 2006). Ratios of 5% damped response spectra of strong motion records were used in this study instead of Fourier spectral ratios commonly used in the receiver functions method. Essentially based on amplitudes and shapes of HVSR, the technique was developed for assigning site classes to the K-Net strong motion stations, in order to confer a reliable modelling of site effects to the Japanese attenuation models. One of the remarkable conclusions of the author was the amplitude of H/V ratios may not be appropriate for assessing amplification potential of an engineering site and for estimating loads to which structures could be exposed.

Ghasemi *et al.* (2009) classified 107 strong motion stations of the Iranian Strong Motion Network, following three different empirical schemes. Firstly, stations with site classes previously determined by local geological conditions and $V_{s,30}$ measurements are reclassified using recorded strong motion at each station. In this regard, the average H/V spectral ratio of records at each station is determined, and then, the period of the first predominant peak is taken as the site natural period. The same conclusions as those made by Zhao (2006) were obtained in this study, in particular, the incapacity of these empirical classification techniques to account for special features of site effects. A new site classification approach was also suggested by Saman and Tsang (2011), based on artificial neural networks. The mean HVSR curves proposed by Zhao (2006) were considered to classify 87 strong motion stations with previously known local conditions, based on the Chi Chi Taiwan strong motion records.

In this study an alternative tool is proposed to characterize design sites classified in the Algerian seismic building code (RPA99/ver 2003, herein referred to simply as RPA99) by average transfer functions through a stochastic approach combined to a statistical study. Unlike response spectra, transfer function is a powerful mathematical means for site effects assessment. It allows a direct and full characterization of soil profile by its vibration frequencies and, especially, its amplification capacity. For each RPA99 soil class, the deterministic average transfer function is calculated on a wide sample of one dimensional layered soil profiles, where, the average S-W velocity, V_s, in any layer is simulated using the random field theory.

V_s is a positive-unbounded parameter and is supposed to be governed by a lognormal distribution. However, for each layer of a RPA99 design site, V_s is bounded above and below (Table 1) and neither the normal nor the lognormal distributions are then appropriate. For this reason, a probabilistic model accounting for bounded distributions is used. The results obtained in this study indicate that the present approach provides an accurate site identification tool and gives a reliable measure of the amplification capacity and the corresponding frequency ranges. The average transfer functions are then used to compute the average site factor for each site class following the Eurocode (EC8) provisions. Average normalized response spectra for all RPA99 design sites are also calculated and the amplification influence is investigated through their combination with the corresponding site factors previously calculated.

Table 1 RPA99 site categories

Site type	Geotechnical description	Mean value of V_s (m/s)
S1	Rock site:	
	Rock or other similar geological formation	$V_s \geq 800$
S2	Stiff site:	
	Deposits of dense sand, gravel and/or over consolidated	$V_s \geq 400$
	clay with 10 to 20 m thickness	From 10 m thickness
S3	Soft site:	
	Deep deposits of medium dense sand, gravel or medium raid clay	$V_s \geq 200$
		From deep of 10 m
S4	Very soft site:	
	Deposits of releases sand with/without presence of soft clay layers	$V_s < 200$
		In firsts 20 m

2 Brief review of site effects consideration in the RPA99

The northern part of Algeria is a moderate-to-strong seismic region as evidenced by recent seismic events(CRAAG, 1994; Benouar, 1994; Bouhadad and Laouami, 2002), the last one being the Boumerdes earthquake which occurred in May 21, 2003, M_w=6.8. Many sites in this area have topographic, geological and geotechnical conditions that favour local effects (Laouami *et al*., 2006; Laouami and Slimani, 2013). In RPA99 the amplification phenomenon is indirectly considered through normalized response spectra corresponding to four soil categories, where the site coefficient concept is not clearly included (Table 1 and Fig. 1). Moreover, to avoid the resonance phenomenon, this code recommends that particular caution should be paid to the building site (RPA99 Sec. 2.1).

3 Methodology for the transfer function calculation

The researches on site seismic classification reviewed above demonstrate that the reliability of a classification scheme is vital for seismic hazard studies. However, in seismic design of structures, the concern of engineers is to quantify forces and/or displacements to which structures might be exposed. In this regard, attributing a class to a particular engineering site according to a certain design code cannot by itself be sufficient even when the classification is suitable. To address this concern, the mean transfer function is proposed as a simple tool to ensure an appropriate site classification and a consistent assessment of its amplification capacity. The transfer function is a mathematical means governing the input/output relationship of a physical system in the frequency domain. It is defined in this study as the ratio of the surface motion amplitude to rock outcrop motion amplitude. This new site classification method has many advantages which are not likely provided by classical methods cited previously (S-W velocity profile, mean HVSR schemes, predominant period, and so on), because it makes possible the estimation of the expected ground surface responses representing the actual excitations acting on the structures. This protects against deficiencies related to bad estimation of the local effects, which are often neglected, underestimated or overestimated. The response spectrum computed via average transfer function is moreover compatible with local site conditions and accounts correctly for the influence of the site's amplification. Thus, for a site with unknown S-W velocity profile, the natural frequency can easily be determined by the micro-tremor HVSR method. The corresponding site class is then derived by putting the natural frequency on the appropriate average transfer function curve. For strong motion stations the natural frequency is derived from the mean HVSR of records and the site class is assigned by the same manner as cited above.

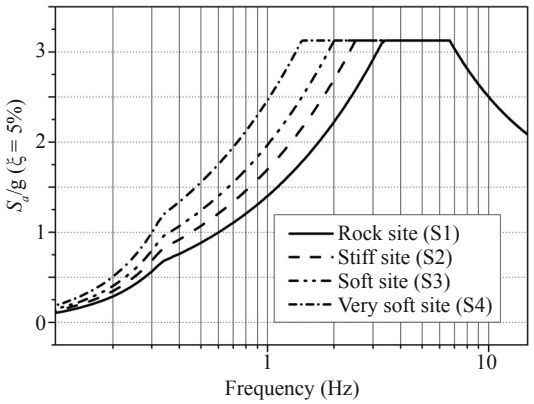

Fig. 1 Normalized acceleration design response spectra - RPA99

An average transfer function is proposed for each RPA99 design site excepting the rock site (S1), which is supposedly unaffected by the amplification effects and taken as a reference site. Nevertheless, with not enough information on subsurface geological settings, the data on V_s can be scarce. For that reason, 1-D soil profiles have been performed through a random simulation for all RPA99 design sites, except for the rock site (S1). The simulated soil profiles are all representative of the concerned design site in terms of average V_s values and thicknesses of the different layers.

V_s is in general an unbounded positive parameter; its variability is often modelled as a lognormal distribution. However, since the average V_s for any layer of each RPA99 design site is between two boundary values, it is a bounded positive parameter. A probabilistic model that maps an unbounded distribution of V_s to a bounded one has been used (Fenton and Griffiths, 2000). It arises from a simple transformation of an average local and standard random field having zero mean and unit variance. Consequently, for each soil layer, a sample of one thousand (1000) average S-W velocity values is simulated with respect to the recommended requirements of RPA99. The process starts with the stochastic simulation of normally distributed random fields having zero mean and unit variance (Fig. 2), which are then used to compute the average S-W velocity profiles following the relationship:

$$\overline{V}_i^j = \overline{V}_{i\min}^j + \frac{1}{2}(\overline{V}_{i\max}^j - \overline{V}_{i\min}^j)\left[1 + \mathrm{th}\,(s\frac{\Delta\overline{v}_i^j}{2\pi})\right] \quad (1)$$

where $\overline{V}_{i\min}^j$ and $\overline{V}_{i\max}^j$ are the minimal and maximal bounds of the average S-W velocity in *i*th layer of *j*th soil profile, respectively; th(.) is the hyperbolic tangent; $\Delta\overline{v}_i^j$ is a local and standard random field having zero mean and unit variance and *s* is a factor governing the

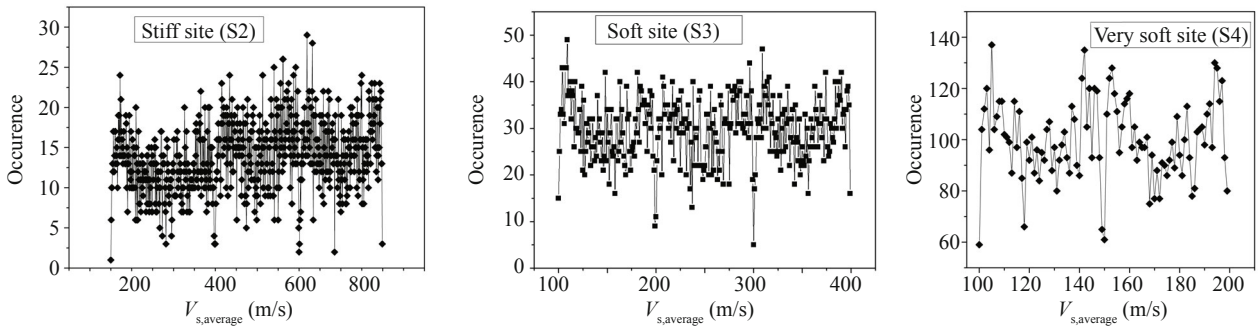

Fig. 2 Simulation results of average S-W velocity for S2, S3 and S4 sites presented under the form of occurrence of mean V_s values

mean S-W velocity variability between its two bounds, and

$$\Delta\overline{v}_i = \frac{2}{N}\sum_i \cos(2\pi\varphi_i)^{\frac{1}{2}} \tag{2}$$

where, ϕ_i is a random number and N the number of elements in the summation. The average transfer function for linear viscous-elastic model in frequency domain is obtained by calculating the arithmetic mean of transfer function values. The standard deviation is also performed for any mean amplification value corresponding to a given frequency. For the record, we found no noticeable variation of the average transfer function for sample sizes beyond 1000 profiles,

3.1 Nonlinearity effects

It is commonly recognized that soil deposits behave nonlinearly over strong motions near the surface. In this study, the soil's dissipative character is considered to approximate the nonlinear response of soil deposits. This is due to the decrease in the elastic shear modulus values, G, and the increase in damping values, β, under strong motions. However, with little available data on G and β variations, these so-called reduction curves were taken from the literature (Seed and Idriss, 1970; Seed and Sun, 1989). The reduction curves were selected according to the dissipation level which varies following the soil mechanical properties. Rock time-histories collected from European Strong Motion (ESM) database (Ambraseys *et al*., 2002) and PEER Strong Motion (PSM) database (http://peer.berkeley.edu/smcat/) (Fig. 3) were used as input motion through 1-D equivalent linear soil seismic analysis conducted by a developed computer program. European records extracted from the ESM database are uniformly processed by filtering between 0.25 and 25 Hz, while records from PSM database has a useable bandwidth within 1/1.25 of the low pass frequency and 1.25 of the high pass frequency. The ground surface response was computed first and the strain was derived and used to determine final G and β values following an iterative process. Then, the equivalent linear transfer function for any simulated soil profile is calculated.

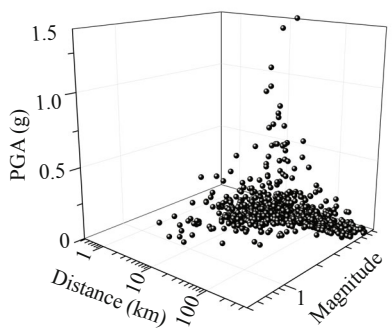

Fig. 3 Distribution of events considered in this study according to magnitude, epicentral distance and PGA

4 Discussion of results

The average transfer function curves and their evolution in frequency range in both linear and equivalent linear cases are illustrated in Fig. 4. The first peaks (Figs. 4(a), 4(c) & 4(e)) highlight fundamental modes that characterize the respective sites and bring out their corresponding fundamental frequencies and amplification levels. These two parameters (fundamental frequency and amplification level) vary according to the S-W velocity changing when observing the overall shape of transfer function curves. Also, peak amplification levels increase significantly from high frequencies (S2) to low ones (S4). Additionally, it is clearly noted that the S-W velocity tends to vary depending on the mechanical properties associated with the site's consistency, which is, overall, stronger for stiff soils and moderate for soft and very soft soils.

It is clear from Fig. 4(b) that transfer function curves of the stiff site (S2) show a common amplification peak at 5.17 Hz in both the linear and equivalent linear cases. The curves are almost identical if the slight difference in the maximal amplitude evidenced by the two amplification peaks is excluded. This confirms the absence of nonlinearity effects, a characteristic of firm and rock sites. The average transfer function curves of S3 sites reveal amplification peaks at 2.34 Hz and 2.24 Hz for the linear and equivalent linear cases, respectively (Fig. 4(d)). The appearance of those two peaks at different frequency values is due to nonlinear behaviour; soft sites are less consistent than stiff sites,

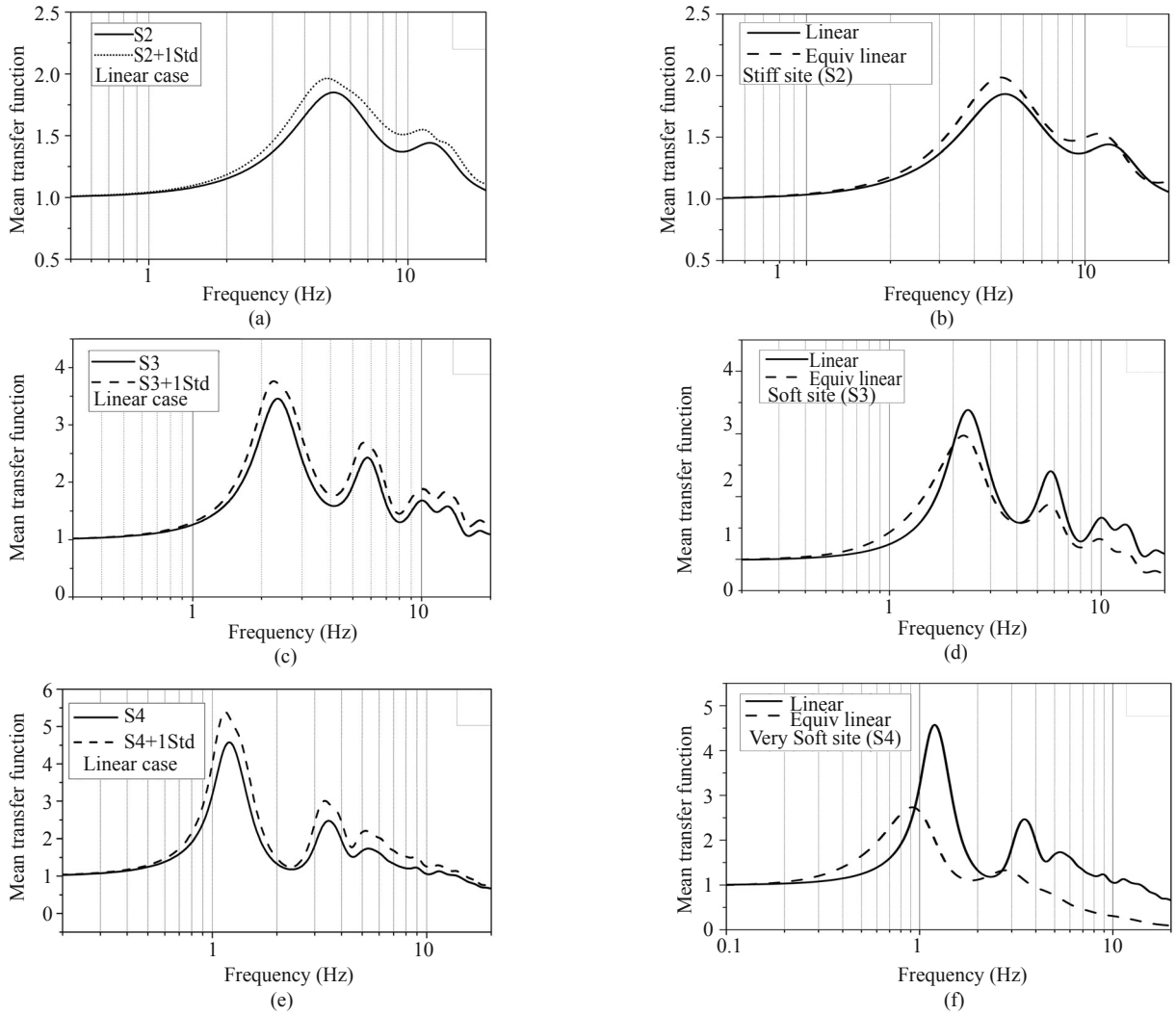

Fig. 4 Average transfer functions for RPA99 S2, S3 and S4 sites in linear and equivalent linear cases. The average transfer function plus one standard deviation in the linear case is also presented for each site class.

and as a result, a beginning of nonlinearity effects under strong ground motions is observed. From the overall shape of the soft site transfer function curves, it can be observed that the peak frequencies for the linear and equivalent linear cases are different. The peak frequency in the equivalent linear case is, in fact, shifted toward lower frequencies. Also, in both the linear and equivalent linear cases, the peak's narrowness is more evidenced, in contrast to stiff sites where the transfer function peaks are relatively broad. Because of the disproportionally higher damping (the shaking ground motion dependency on the soil consistency), the nonlinear behaviour is characterized mainly by a decrease in the amplification level and the resonance frequency. For this reason, the S4 site seems strongly affected by nonlinearity effects as evidenced by the difference in the amplitudes in the linear and equivalent linear cases, viz., 4.57 and 2.73, respectively (see Table 2 and Fig. 4(f)). Additionally, the peak frequency is shifted slightly to a lower value

Table 2 Amplification values and corresponding frequencies in linear and equivalent linear cases

Site	Frequency (Hz)		Amplification	
	Linear	Equivalent linear	Linear	Equivalent linear
S2	5.17	5.00	1.81	1.91
S3	2.34	2.24	3.45	2.24
S4	1.19	0.90	4.57	2.73

(0.9 Hz) as compared to the 1.19 Hz for the linear case.

5 Classification tests

Two site classification tests according to RPA99 provisions are performed based on the resonance frequency of the concerned site and mean transfer functions previously computed. The main goal here is to check the reliability and the effectiveness of the average transfer functions in assigning site class to a given design site. This step is of a great importance in engineering structure design, since it leads to a response spectrum and amplification factor that reflect local site conditions and are appropriate to the structural type of interest.

The first classification test considers 120 sites from the Kik-Net Japanese database (http://www. kik. bosai.go.jp/), with previously determined S-W velocity profiles (Table 3). The sites are classified first following the RPA99 site classes, i.e., considering the average S-W velocities in soil layers. The transfer function of each site is thereafter computed to extract the fundamental frequency. In the proposed average transfer function curves, each site class ranges within the frequency interval bounded by the fundamental peak intersection points of two consecutive transfer function curves (Fig. 5). For every Kik-Net site, the fundamental frequency is extracted from the transfer function curve primary peak and then used to attribute a site class by positioning it on the appropriate average transfer function curve. Table 3 shows comparison between the RPA99 site classification based on the S-W velocity profiles (Table 3 and Fig. 5) and site classes assigned according to the proposed mean transfer function (MTF) method. Of the 120 sites, 86 were successfully classified which means that classes assigned with the MTF method provide a reasonably good success rate (71.7%) compared with the pre affected RPA99 classes. It is also noted that except for site N° 70, MTF site classes within ±1 class are completely successful compared with the other classification.

The proposed classification method has also been applied to a number of sites situated in the Mitidja basin (central northern part of Algeria). The Mitidja basin is part of the Tell Atlas, an east-northeast-trending, fold-and-thrust belt along the plate boundary in North Africa. Laouami and Slimani (2013) studied earthquake induced site effects during the 2003, 21 May Boumerdes (Algeria) earthquake through damages on the built structures and their relationship with soil spectral ratios. Micro-tremor and strong motion H/V spectral ratio curves were performed at four locations in the Mitidja basin (Table 4), where S-W velocity profiles are available. Hence, S-W velocity profiles based classification can initially be made according to RPA99 provisions. In this section, results found by Laouami and Slimani (2013) are used as local soils with well defined S-W velocity profiles are very limited. Ambient noise H/V curves are particularly used in order to extract fundamental frequencies, since it is largely accepted among researchers that H/V spectral ratio curves give a good estimation of the soil fundamental frequency. Indeed, Kawase *et al*. (2011) has developed a new formulation based on the theory of diffuse field for plane waves and demonstrated the relationship between the H/V amplification function and the transfer function of a soil profile. This relationship shows that H/V function is proportional to the ratio of the horizontal to vertical transfer functions and a coefficient which is the ratio of P wave (Love wave) and S-W velocities. Also, the study confirmed the perfect correspondence of the peak frequencies between the H/V amplification function and the transfer function curves.

The sites are firstly classified on the basis of their S-W velocity profiles made by the Japan International Corporation Agency (JICA) with the cooperation of Earthquake Engineering Research Centre (CGS, Algeria) (JICA and CGS, 2006) (Fig. 6), and then, they are reclassified by the way of mean transfer function curves through the fundamental frequency value.

For the Boumerdes site, the RPA99 class derived from the S-W velocity profile is S2 class (firm site V_s> 400 m/s from 10 m depth), while the plotted ambient noise H/V curve obtained for this site shows a smooth bump in the 0.8 to 1.2 Hz frequency range (Fig. 7), and another peak around 4 Hz. There are two possibilities for classifying this site. The first one considers the peak around 1 Hz, and so it will be S4. But in this case, the very low amplification demonstrates the lack of clear contrast with the bedrock, which makes this classification unlikely. Alternately, consider the peak around 4 Hz, and in this case, the site would be classified S2 as the frequency is between 3.75–7 Hz within the S2 mean transfer function curve. Furthermore, clear velocity contrast had already been shown at 12 meters and its average velocity was around 240 m/s (Fig. 6(c)), which indicates a resonance frequency around 5 Hz according to $f = V_s / 4h$. But the deeper velocity structure wasn't obvious and it was possible that another big velocity contrast in deeper bedrock might exist and generate a 1 Hz peak.

For the Dar El Beida site, the micro-tremor H/V curve shows a clear peak at around 4 Hz frequency representing the site fundamental frequency (Fig. 8). This allows assigning S2 class ranging from frequencies greater than 3.76 Hz in the proposed S2 mean transfer function curve (Fig. 5). Furthermore, the S-W velocity profile of the Dar el Beida site (Fig. 6(b)) leads to the same site class (S2 class), which is attributed in reference to RPA99 provisions, since the mean V_s value is larger than 400 m/s at 10m depth (Table 1).

The flattening of the plotted micro-tremor H/V spectral ratio curve of the Hussein Dey site (Fig. 9) shows that a fundamental peak is not clearly evident which is indicative of firm-to-rock soil characteristics. The fundamental frequency cannot be accurately identified even if information extracted from the plotted curve shape confirms presence of firm-to-rock site, what is also

Table 3 Results of the Kik-Net site classification test. The table gives the mean transfer function based classification and the one made according to RPA99 provisions. f_1 and f_2 are the band frequency limits defining the site class. The second column of the table indicates the site's reference as given by the Kik-net database

N° profile	Ref	$V_{s,10}$ (m/s)	$V_{s,20}$ (m/s)	$V_{s,30}$ (m/s)	f_1 - f_2 (Hz) Mean transfer functions				RPA99 Class	Mean TF Class
					S1	S2	S3	S4		
					> 7	3.76–7	1.53–3.75	<1.53		
					f_0 (Hz) soil profile					
1	ABSH03	255.3		499.16		4.87			S3	S2
2	ABSH05	345.6		624.3		4.87			S3	S2
3	ABSH07	187.5	242.4	290.3		1.75			**S3**	**S3**
4	ABSH08	325		517.4		2.75			**S3**	**S3**
5	ABSH09	237.9		394.2		1.25			S3	S4
6	ABSH13	324		463.6		2.75			**S3**	**S3**
8	ABSH14	235.7		351.6		1.87			**S3**	**S3**
7	ABSH15	448.7		464.5		2.12			S2	S3
9	AICH05	237.4		301.3		0.75			S3	S4
10	AICH06		197.3	219.4		1.25			**S4**	**S4**
11	AICH12		156.0	163.2		1.12			**S4**	**S4**
12	AICH14		139.6	154.2		0.75			**S4**	**S4**
13	AKTH12	208.3		389.2		2.87			S3	S3
14	AOMH13		139.8	154.0		0.75			**S4**	**S4**
15	AOMH14	187.5	293.0	360.0		2.75			**S3**	**S3**
16	AOMH15	336.4		577.5		2.75			**S3**	**S3**
17	AOMH16		196.5	225.7		1.00			**S4**	**S4**
18	AOMH17	226.2		378.3		2.60			**S3**	**S3**
19	AOMH18	189.8	289.5	369.1		3.75			**S3**	**S3**
20	CHBH06	189.4	203.4	237.8		0.62			S3	S4
21	EHMH01	420		743.4		6.62			**S2**	**S2**
22	EHMH04	150	216.6	254.0		2.00			**S3**	**S3**
23	FKIH02	220.1		342.8		3.00			**S3**	**S3**
24	FKIH04	300		300.0		1.62			**S3**	**S3**
25	FKIH06	235		395.0		2.00			**S3**	**S3**
26	FKOH03	302.1		431.8		5.75			S3	S2
27	FKOH08	271.2		535.7		5.25			S3	S2
28	FKSH04	204		246.0		2.50			**S3**	**S3**
29	FKSH18	251		307.0		3.37			**S3**	**S3**
30	FKSH19	241		338.0		3.12			**S3**	**S3**
31	GIFH05	146	210.4	262.0		3.00			**S3**	**S3**
32	GIFH13	430.5		592.6		1.62			S2	S3
33	GIFH14	440		627.3		4.75			**S2**	**S2**
34	GIFH17	250		429.4		4.37			S3	S4
35	GIFH18	353.7		553.0		5.87			S3	S2
36	GIFH25	357.1		468.7		2.62			**S3**	**S3**
37	GNMH01	421		293.7		1.87			**S3**	**S3**
38	HDKH01	206.4		368.2		4.37			S3	S2
39	HDKH04	186	210	235.0		1.37			S3	S4
40	HDKH05	493		766.2		6.75			**S2**	**S2**
41	HDKH06	280		412.2		3.87			**S3**	**S3**
42	HDKH07	348.3		459.0		3.25			**S3**	**S3**
43	HDKH09	194.7	292	364.0		3.62			**S3**	**S3**
44	HRSH02	181	294.6	390.7		4.87			S3	S2
45	HRSH06	208.6		279.1		2.50			**S3**	**S3**

N° profile	Ref	$V_{s,10}$ (m/s)	$V_{s,20}$ (m/s)	$V_{s,30}$ (m/s)	f_1 - f_2 (Hz) Mean transfer functions (Hz) soil profile				RPA99 Class	Mean TF Class
					S1 > 7	S2 3.76–7	S3 1.53–3.75	S4 <1.53		
46	HRSH07	558.7		461.4		2.50			S2	S3
47	HRSH14	394.2		550.1		4.12			S3	S2
48	HYGH07	290.5		415.5		6.125			S3	S2
49	HYGH08	158	224.1	260.5		3.12			**S3**	**S3**
50	HYGH09	194.7	292	364.4		3.5			**S3**	**S3**
51	HYGH10	169.2	207.1	223.8		1.25			S3	S4
52	HYGH13	235.3		381.3		3.25			**S3**	**S3**
53	HYGH15	280.0		526.0		3.75			**S3**	**S3**
54	HYMH01	261.5		395.0		1.87			**S3**	**S3**
55	HYMH02	364.0		497.6		3.00			**S3**	**S3**
56	IBUH01	248.0		306.0		2.37			**S3**	**S3**
57	IBUH02	309.8		541.8		5.50			S3	S2
58	IBRH11		197.0	242.4		2.50			S4	S3
59	ISKH03	171.8	255.8	297.2		3.75			**S3**	**S3**
60	ISKH04	440.0		443.0		4.87			**S2**	**S2**
61	ISKH05	435.0		681.0		4.75			**S2**	**S2**
62	ISKH08	411.7		635.8		4.50			**S2**	**S2**
63	IWTH08	207.9		304.5		3.00			**S3**	**S3**
64	IWTH12	252.5		367.9		1.87			**S3**	**S3**
65	KGSH01	510.3		602.9		1.87			S2	S3
66	KGSH03	910.0		1196		8.25			**S1**	**S1**
67	KGSH04	233.03		280.4		1.75			**S3**	**S3**
68	KGSH09	320.0		409.0		2.75			**S3**	**S3**
69	KGWH02		161.3	185.3		1.50			**S4**	**S4**
70	KGWH04	196.8	299.3	407.2		8.25			S3	S1
71	KKWH02	540.3		656.9		2.37			S2	S3
72	KKWH04	237.0		372.0		1.62			**S3**	**S3**
73	KKWH10	194.1	271.2	327.5		2.87			**S3**	**S3**
74	KKWH11	170.0	212.5	242.8		2.12			**S3**	**S3**
75	KKWH15	307.0		528.6		2.87			**S3**	**S3**
76	KMMH12	316.9		409.7		1.50			S3	S4
77	KMMH14	143.4	200	248.2		1.25			**S4**	**S4**
78	KMMH15	355.5		499.8		3.12			**S3**	**S3**
79	KNGH18	304.4		388.4		3.00			**S3**	**S3**
80	KNGH19	456.5		701.0		8.70			S2	S1
81	KOCH03	441.1		668.2		5.25			**S2**	**S2**
82	KOCH011	600.0		782.2		5.37			**S2**	**S2**
83	KOCH12	358.6		496.3		2.87			**S3**	**S3**
84	KSRH04		162.8	189.1		1.12			**S4**	**S4**
85	KSRH07		160.3	204.0		1.37			**S4**	**S4**
86	KSRH09		185.9	230.0		1.62			S4	S3
87	KYTH04	205.8		240.1		2.00			**S3**	**S3**
88	KYTH04	762.3		1068.9		7.25			S2	S1
89	KYTH05		110	133.15		1.00			**S4**	**S4**
90	MIEH01	196.8	280	342.0		3.25			**S3**	**S3**
91	MIEH02	218.0		423.0		2.87			**S3**	**S3**
92	MIEH03	231.0		434.0		5.50			S3	S2

N° profile	Ref	$V_{s,10}$ (m/s)	$V_{s,20}$ (m/s)	$V_{s,30}$ (m/s)	f_1 - f_2 (Hz) Mean transfer functions				RPA99 Class	Mean TF Class
					S1	S2	S3	S4		
					> 7	3.76–7	1.53–3.75	<1.53		
					(Hz) soil profile					
93	MIEH04	280.4		342.0		3.25			**S3**	**S3**
94	MIEH08	603.0		1009.7		6.75			**S2**	**S2**
95	MYGH08	281.2		358.2		2.12			**S3**	**S3**
96	NGNH24	345.9		464.2		1.62			**S3**	**S3**
97	NGNH26	243.7		300.4		1.25			S3	S4
98	NGNH29	266.6		465.0		2.12			**S3**	**S3**
99	NGNH30	247.5		456.0		3.75			**S3**	**S3**
100	NGNH31	322.7		706.7		1.62			**S3**	**S3**
101	NGNH54	600.0		661.3		4.75			**S2**	**S2**
102	NIGH02	300.0		360.0		2.12			**S3**	**S3**
103	NIGH04	287.0		392.0		1.62			**S3**	**S3**
104	NIGH08	269.2		326.8		0.62			S3	S4
105	NIGH09	300.0		463.0		2.75			**S3**	**S3**
106	NIGH14	320.0		437.6		3.37			**S3**	**S3**
107	NIGH18	229.7		311.0		2.37			**S3**	**S3**
108	RMIH02		141.8	154.9		1.12			**S4**	**S4**
109	RMIH04	456.7		543.0		2.50			S2	S3
110	SBSH09	549.4		719.1		4.50			**S2**	**S2**
111	SMNH11	500.0		670.0		6.00			**S2**	**S2**
112	SOYH02		117.6	118.4		0.87			**S4**	**S4**
113	SOYH08	320.0		533.3		3.75			**S3**	**S3**
114	SOYH09	270.0		244.0		1.87			**S3**	**S3**
115	SZOH35		122.5	158.3		1.12			**S4**	**S4**
116	TKCH03	214.3		372.4		1.50			S3	S4
117	YMTH05	416.4		533.1		2.12			S2	S3
118	YMTH03	667.0		899.8		4.75			S2	S3
119	YMGH01	1000.0		1387.6		7.25			**S1**	**S1**
120	TKCH07		121.8	140.1		1.12			**S4**	**S4**

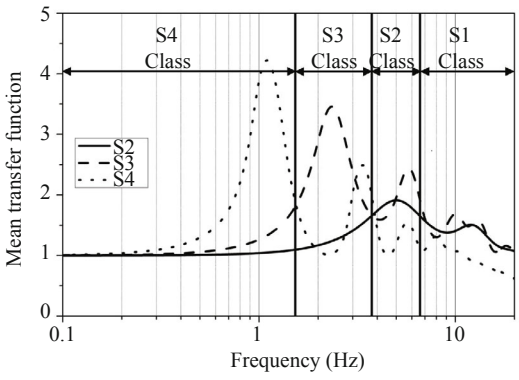

Fig. 5 Frequency range boundaries of S1, S2, S3 and S4 soil classes. The S1 class is defined for frequencies greater than 7 Hz. The S2 class ranges between 3.76 Hz and 7 Hz frequencies, whereas the S3 class rages within the frequency interval of 1.53 to 3.76 Hz. The S4 class is included in the frequency range set by the value of 1.53 Hz

supported by the S-W velocity profile of this site (Fig. 6(a)). In that case, the V_s mean value of about 700 m/s is reached at a depth less than 10 m indicating then firm-to-rock nature of the Hussein Dey site according to RPA99 dispositions.

The micro-tremor H/V spectral ratio curve of the El Affroun site (Fig. 10) shows a clear peak at a frequency slightly greater than 3 Hz, indicating the site's fundamental frequency. This frequency corresponds to S3 class, according to the S3 mean transfer function curve (Fig. 5), in agreement with the quaternary soft deposits of the Mitidja basin where the site is located. It should be noted that further studies and more information such as a S-W velocity profile are needed to make a reliable classification of the El Affroun site.

The proposed classification method has been tested for 120 Kik-net database sites having defined S-W velocity profiles and the result has been compared with

Table 4 Geographical coordinates of the sites considered in the second test classification (Laouami and Slimani, 2013)

Site coordinates	Hussein Dey	El Affroun	Dar ElBeida	Boumerdes
Latitude	36.74°	36.469°	36.716°	36.756°
Longitude	3.096°	2.632°	3.206°	3.473°

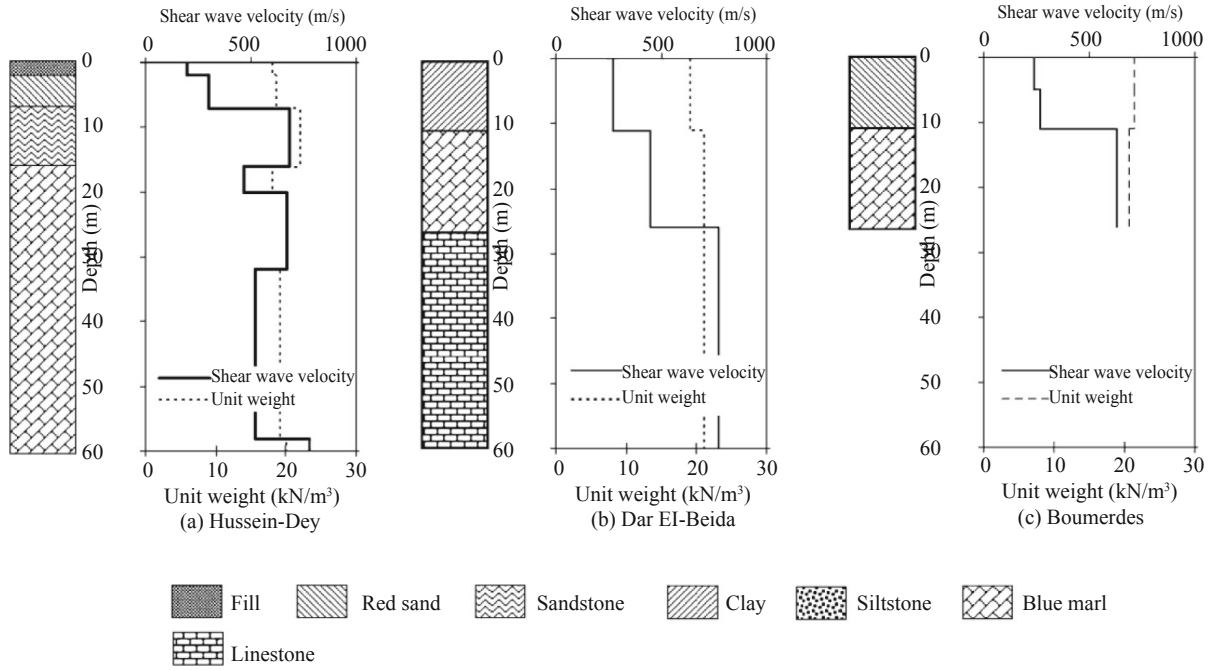

Fig. 6 S-W velocity profiles for three seismic stations: The Hussein Dey, the Dar El Beida and the Boumerdes sites (JICA and CGS, 2006 from Laouami and Slimani, 2013)

the RPA99 based classification. This test provides a success rate of 71.7% (Table 3). Site classifications have also been made for local sites located in the Mitidja basin through micro-tremor H/V spectral ratio curves performed by Laouami and Slimani (2013), and then compared with those derived from available S-W velocity profiles (Fig. 6). The obtained results show that in the absence of S-W velocity profiles, the proposed method combined with a micro-tremor measure offers a good tool for soil classification.

6 Site amplification factors (SF)

The site amplification factor represents the ground motion amplification with respect to outcrop conditions. It is obtained by the ratio between the peak ground acceleration (PGA) at the site surface and the one at the engineering bedrock (reference site). The site factor is considered as a useful and reliable means capable to report on the amplification potential of a given engineering site.

For practical design purposes, RPA99 provides acceleration values called zone's acceleration coefficients, estimated at the bedrock (Table 5). Currently, RPA99 proposes design elastic response spectra which clearly do not integrate the concept of the site amplification factor. Indeed, all the plotted elastic response spectra shapes show the same horizontal plateau level, although they represent different soil classes (Fig. 1).

In this part of the study, an attempt is made to compute average site factors and average elastic response spectra based on mean transfer functions previously calculated, and then, make a comparison with the current EC8 design site factors. Moreover, the resulting site factors will be compared with those found by Pitilakis *et al*. (2012) which are proposed to be introduced in the next

Table 5 Seismic zone coefficients (RPA99)

Building type group	Seismic zone			
	I	IIa	IIb	III
1A	0.15	0.25	0.30	0.40
1B	0.12	0.20	0.25	0.30
2	0.10	0.15	0.20	0.25
3	0.07	0.10	0.14	0.18

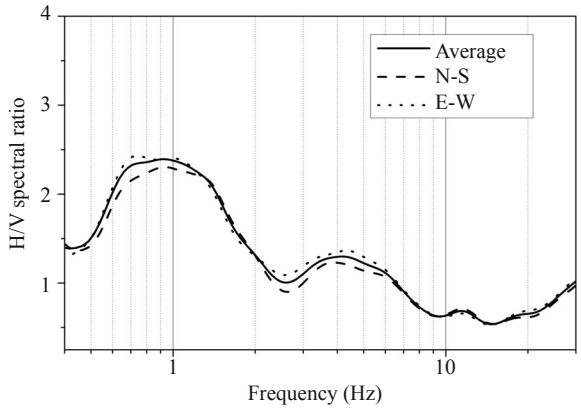

Fig. 7 North–South, East–West and average H/V spectral ratios for micro-tremor at the Boumerdes site (Laouami and Slimani, 2013)

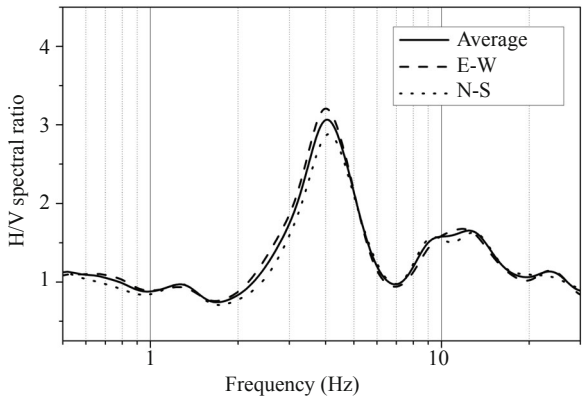

Fig. 8 North–South, East–West and average H/V spectral ratios for micro-tremor at the Dar El Beida site (Laouami and Slimani, 2013)

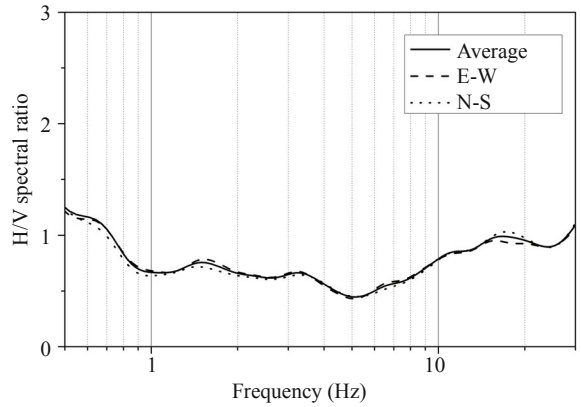

Fig. 9 North–South, East–West and average H/V spectral ratios for micro-tremor at the Hussein Dey site (Laouami and Slimani, 2013)

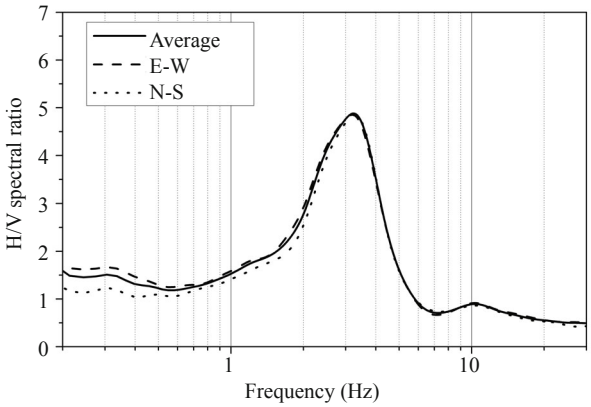

Fig. 10 North–South, East–West and average H/V spectral ratios for micro-tremor at El Afroun site (Laouami and Slimani, 2013)

EC8 amendment. The calculated response spectra will also be discussed and compared with the corresponding design response spectra of RPA99 and EC8, respectively. Except for the S1 class representing the rock site, average site factor is calculated for each site class by:

$$\gamma_r(f) = \mathrm{TF}^{-1}(\gamma_r(t)) \tag{3}$$

$$\gamma_s(f) = H(f).(\gamma_r(f)) \tag{4}$$

$$\gamma_s(t) = \mathrm{TF}^{-1}(\gamma_s(f)) \tag{5}$$

where, $\gamma_r(t)$ and $\gamma_s(t)$ are the acceleration records at the base and the surface in the time domain, respectively; $\gamma_{r\,max}$ and $\gamma_{s\,max}$ are the maximal accelerations at the base and the surface respectively; $\gamma_r(f)$ and $\gamma_s(f)$ are the acceleration records at the base and the surface in the frequency domain, respectively; $H(f)$ is the transfer function between the rock basement and the soil surface and TF^{-1} is the inverse Fourier transform. The site factor, SF, is given by:

$$\mathrm{SF} = \frac{\gamma_s(t)_{max}}{\gamma_r(t)_{max}} \tag{6}$$

The calculation procedure has been made according to EC8 provisions, i.e., considering two levels of seismic action, Type1 and Type 2 (EC8, section 3.2). According to EC8, it should take into account the magnitude of the earthquakes that contribute mainly to the seismic hazard defined for the probabilistic assessment of the hazard, rather than conservative upper limits (e.g., maximum credible earthquake).

Site factors and accompanying elastic response spectra of Type 1 should be used when the earthquake contributing to the seismic hazard has a surface wave magnitude, M_s, greater than 5.5. These response spectra have more energy at low frequencies and should be used in regions with high seismic activity. Conversely, the Type 2 elastic response spectra are proposed for earthquakes with $M_s \leq 5.5$, having larger spectral amplitudes at high frequencies. To reach that objective, the accelerometer records previously used have been divided into two

datasets based on M_s 5.5. For each record, the Fourier spectrum was computed and then convoluted with the average transfer function of the concerned site, to obtain signal at the surface site incorporating the particular distinctive features such as the frequency content and the amplification potential. The site factor is then obtained through the ratio between the PGA at the surface and that at the rock basement (Eqs (3)-(6)). The mean site factor and its standard deviation are also computed for both considered record datasets representing the two specified seismicity levels.

6.1 Average site factors

Direct simplified methods are proposed in EC8 to account for the influence of local conditions on the site seismic response. EC8 considers five subsoil classes A,B,C,D and E, including stratigraphic profile geotechnical descriptions with S-W velocity values at thirty meters depth, $V_{s,30}$ (Table 6). The last class (Class E) is a class with no $V_{s,30}$ values. Two other classes S1 and S2 are to be considered when particular geotechnical investigations are needed (EC8, Table 3.1). Furthermore, various shapes of 5% damped elastic acceleration spectra corresponding to each soil category are considered wherein site effects are directly reflected through the site factor *S*. The input motion intensity is described by the single parameter, a_g, representing the effective peak ground acceleration at rock site (Site Class A) which is taken as a reference site. Both site factors and response spectra are computed for two kinds of wave surface magnitude of records, Type 1 and Type 2 (EC8, Tables 3.2 and 3.3).

As stated earlier, RPA99 categorizes soils into four classes: rock site (S1), stiff site (S2), soft site (S3) and very soft site (S4) (Table 1). The soils are characterized by geotechnical subsoil description, compatible with the geological nature of each site type and average S-W velocity values in layers forming the first thirty meters of the subsoil. For structural design requirements, RPA99 proposes 5% damping elastic acceleration spectrum for each site class, where site effects are not explicitly accounted for (Fig. 1). The peak ground acceleration is obtained via the zone's seismic coefficient depending on the building type (Table 5), multiplied by the acceleration of gravity and is supposed acting at the rock site.

In EC8, the proposed site classes are comparable to the current RPA99 classes in terms of geotechnical description and V_s profile values. One considers that Classes A, B, C and D of EC8 are compatible with S1, S2, S3 and S4 of RPA99 site classes, respectively (Tables 1&6). Obtained results will therefore be compared with the corresponding ones of the Algerian and European seismic codes on the basis of this assumption.

By observing Table 7, it is remarked that for all site classes included in RPA99 the computed average site factors are, in general, consistent with those found by Pitilakis *et al*. (2012). For the type 2 records dataset, site factors computed using the linear average transfer functions are also shown in the table. One supposes that soils show linear behaviour for weak-to-moderate ground motions. In this case, the dissipation of the seismic energy is not as important as in the case of strong ground motions, wherein the shaking amplitude is strongly absorbed by the damping effect. For this second case, equivalent linear mean transfer functions were used, and thus, site factors obtained for the Type 1 records dataset are, overall, smaller than ones found for the Type 2 records dataset. This is related to the nonlinear phenomenon occurred in large magnitude events. This aspect is also valuable for results obtained by Pitilakis *et al*. (2012).

For the Type 2 records dataset, one observes that calculated mean site factors are, in most cases, in good agreement with results found by Pitilakis *et al*. (2012), especially for S2 and S4 sites. Furthermore, S2 mean site factor is significantly close to the one found for the type1 records dataset. That might be justified by

Table 6 Definition of subsoil classes according to EC8

Soil class	Description of stratigraphic profile	$V_{s,30}$ (m/s)
A	Rock or other rock-like geological formation, including at most 5 m of weaker material at the surface	> 800
B	Deposits of very dense sand, gravel, or very stiff clay, at least several tens of meters in thickness and characterized by a gradual increase of mechanical proper ties with depth	360–800
C	Deep deposits of dense or medium-dense sand, gravel, or stiff clay with thicknesses from several tens to many hundreds of meters	180–360
D	Deposits of loose-to-medium non cohesive soil (with or without some soft cohesive layers),or of predominantly soft-to-firm cohesive soil	<180
E	Soil profile consist ingofa surface alluviumlayer with $V_{s,30}$ values of type Cor D, and thickness esvarying between 5 m and 20 m,under lain by stiffer materials with$V_{s,30}$>800m/s	
S1	Deposits consisting or containing a layer at least 10 m thick of soft clays/silts with high plasticity index (PI>40) and high water content	
S2	Deposits of liquefiable soils, sensitive clays, or any other soil profile not included in types A-E or S1	

Table 7 The calculated mean site factors and their standard deviations considering the two seismicity levels for ground motion datasets. The EC8 site factors and those proposed by Pitilakis *et al*. (2012) are also presented in order to enable comparison with results found in this study

Site	$M_s \leq 5.5$ (Type 2)				$M_s > 5.5$ (Type 1)			
	Linear case		EC8	Pitilakis (2012)	Equiv. linear case		EC8	Pitilakis (2012)
	Calculated mean SF	Std			Calculated mean SF	Std		
S2-B	**1.44**	0.05	1.35	1.40	**1.42**	0.067	1.20	1.30
S3-C	**1.70**	0.131	1.50	2.10	**1.65**	0.144	1.15	1.70
S4-D	**1.64**	0.05	1.80	1.80	**1.31**	0.08	1.35	1.35

the good similarity between average transfer functions of S2 site in both linear and equivalent linear cases. For both S3 and C classes, computed site factor values are greater than site factors of S2 and D classes, respectively. The computed site factors of the Type 1 ground motion dataset for all site classes match well with those found by Pitilakis *et al*. (2012). Their values are relatively weak compared with those of the Type 2 record dataset, especially for S4 site, which might explain presence of nonlinear behaviour caused by strong ground motions arising from Type 1 seismicity level. The obtained results underline the low values of the current EC8 site factors for the soil classes B and C.

7 Mean acceleration response spectra

To obtain the mean response spectra curves, acceleration records of both datasets were normalized according to their PGA and used to compute the acceleration pseudo response spectra with 5% damping. For each RPA99 soil class, the obtained mean response spectra are presented in this section. Comparison is then made with the corresponding RPA99 and EC8 design response spectra with and without site factors.

7.1 Comparative analysis

7.1.1Records of Type 2 ($M_s \leq 5.5$)

(a) Stiff site (S2)

The graph of Fig. 11(a) shows the calculated mean acceleration spectrum and the mean plus/minus one standard deviation for S2. The maximal spectral values appear at the 4–10 Hz frequency interval. This is consistent with the near field earthquake characteristics of Type 2 records and stiff soil type. Figure 11(b) shows a comparison of the mean spectrum with the RPA99 S2 design response spectrum with and without site factor. There is a clear difference in the frequency content and also in the spectral amplitudes. The latter is due to the fact that the RPA99 design spectrum is increased by a non-defined constant factor of 1.25 for the four RPA99 spectra. Also, the results show an underestimation of spectral values for the high frequency content ($f > 8$ Hz). Figure 11(c) shows a comparison of the mean spectrum with EC8 B design response spectrum with and without site factor. The results underline a good correlation up to 10 Hz.

(b) Soft site (S3)

The mean S3 acceleration response spectrum has two spectral peaks, at frequencies of 2–3 and 5–6 Hz, respectively (Fig. 12(a)), although one would expect a smooth curve since the mean response spectrum is the average of a large number of events. The appearance of those spectral peaks is most likely influenced by the shape of the S3 mean transfer function curve which exhibits two modes at those frequencies (Fig. 4(d)). As for the S2 site class, a clear difference arises in the spectral amplitude when compared with the RPA99 design spectrum due to the non-defined constant factor of 1.25 affecting the latter (Fig. 12(b)). However, the plateau frequency content is relatively similar for the two curves. On the other hand, comparison results with the EC8 C design spectrum, with and without site factors, underline good similarity for frequency content and spectral amplitudes (Fig. 12(c)).

(c) Very soft site (S4)

The calculated mean response spectrum of S4 site class is presented in Fig. 13(a). The spectrum shape shows two spectral peaks at frequencies of 1–2 and 4–5 Hz, respectively. The appearance of those spectral peaks follows the shape of the S4 mean transfer function curve which exhibits two modes at those same frequencies (Fig. 4(e)). Moreover, the spectral amplitude is larger at frequencies 4-5 Hz because of the Type 2 ground motion (near field) which is characterized by high frequency content (Fig. 13(b)). However, the plateau frequency content is relatively similar for frequencies above 3 Hz. The difference for frequencies below 3 Hz is due to the fact that the RPA99 design spectra do not distinguish between Type 1 and Type 2 ground motions. Comparison with the EC8 D spectrum shown in Fig.13(c) shows good agreement in frequency content as well as amplitude up to 7 Hz frequency, but begs the question of why the EC8 D plateau continues until 10 Hz.

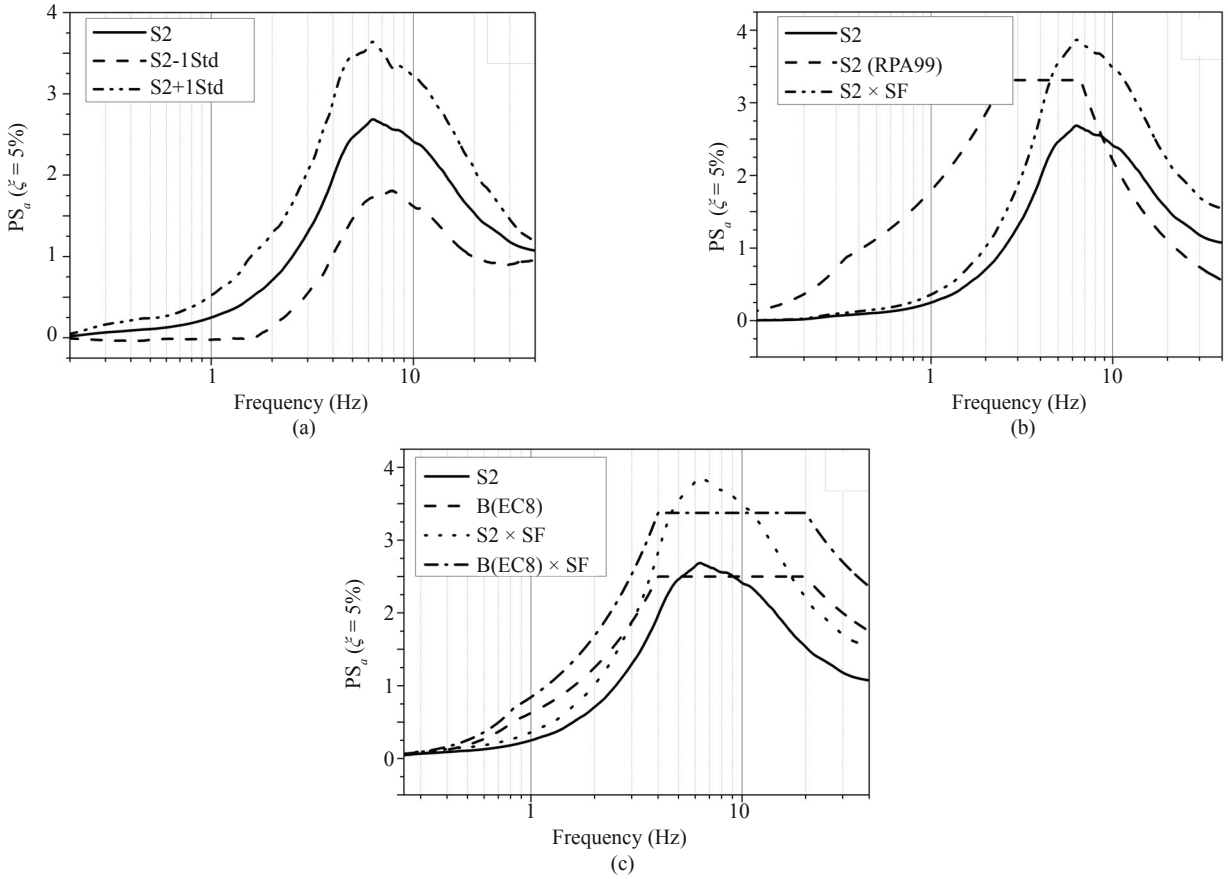

Fig. 11 Mean acceleration pseudo response spectrum with 5% damping of the S2 site. Normalized response spectrum is compared with the corresponding RPA99 S2 and EC8 B design response spectra

7.1.2 Records of Type 1 (M_s>5.5)

(a) Stiff site (S2)

The mean response spectrum for S2 and its plus/minus one standard deviation are presented in Fig. 14(a), which shows a maximal spectral values plateau at the 3–7 Hz frequency range. This frequency range is shifted slightly to the left, i.e., lower frequency values, when compared with the S2 response spectrum for records of Type 1. This is consistent with the characteristics of near field moderate earthquake and stiff soil type. Comparison with RPA99 (see Fig. 14(b)) shows that the two response spectra are in good agreement to 11 Hz. A clear difference in the spectral amplitudes is observed which is due to the non-defined constant factor of 1.25 in RPA99. Figure 14(c) shows a comparison with the EC8 B design response spectra with and without site factor. The results highlight good matching for both spectral values and frequency content, since the spectra are very closer for almost the complete frequency range, even if the S2 site spectrum has somewhat higher maximal spectral values, which can be attributed to the slight difference between the corresponding mean site factors.

(b) Soft site (S3)

The maximal spectral values of the S3 response spectrum are shifted to lower frequencies as compared to the S2 response spectrum (Figs. 15(a) & 14(a)), the high spectral value plateau of S3 being at the 2–3 Hz frequency interval. Moreover, for frequencies lower than 2 Hz, the spectrum shapes seem appreciably consistent but the calculated one remains largely below for the rest of the frequency range. This is because near-field, moderate motion is characterized by low frequency contents. The results indicate a good similarity for the frequency content, also, S3 studied site has a greater amplification level at the high spectral values plateau, which can explain the large deviation between the corresponding site amplification factors (Table 7 and Fig. 15(b)).

(c) Very soft site (S4)

Two spectral peaks at the 1–1.3 Hz range and at 3 Hz frequency, respectively, are prominent in the S4 response spectrum (Fig. 16(a)). The peaks represent good correlation with those of the S4 mean transfer function (Fig. 4(e)). The maximal spectral values of the calculated S4 spectrum are concentrated at lower frequencies in comparison with RPA99 S4 design spectrum (Fig. 16(b)). Additionally the frequency range defining the plateau is relatively similar for the two curves for frequencies above 1.3 Hz. The difference between the curves for frequencies below 1.3 Hz is due to the fact that the RPA99 design spectra do not distinguish between Type 1 and Type 2 ground motions. On the other hand, the spectra shapes highlight a good likeness for the frequency content between the S4 spectrum and the EC8 D

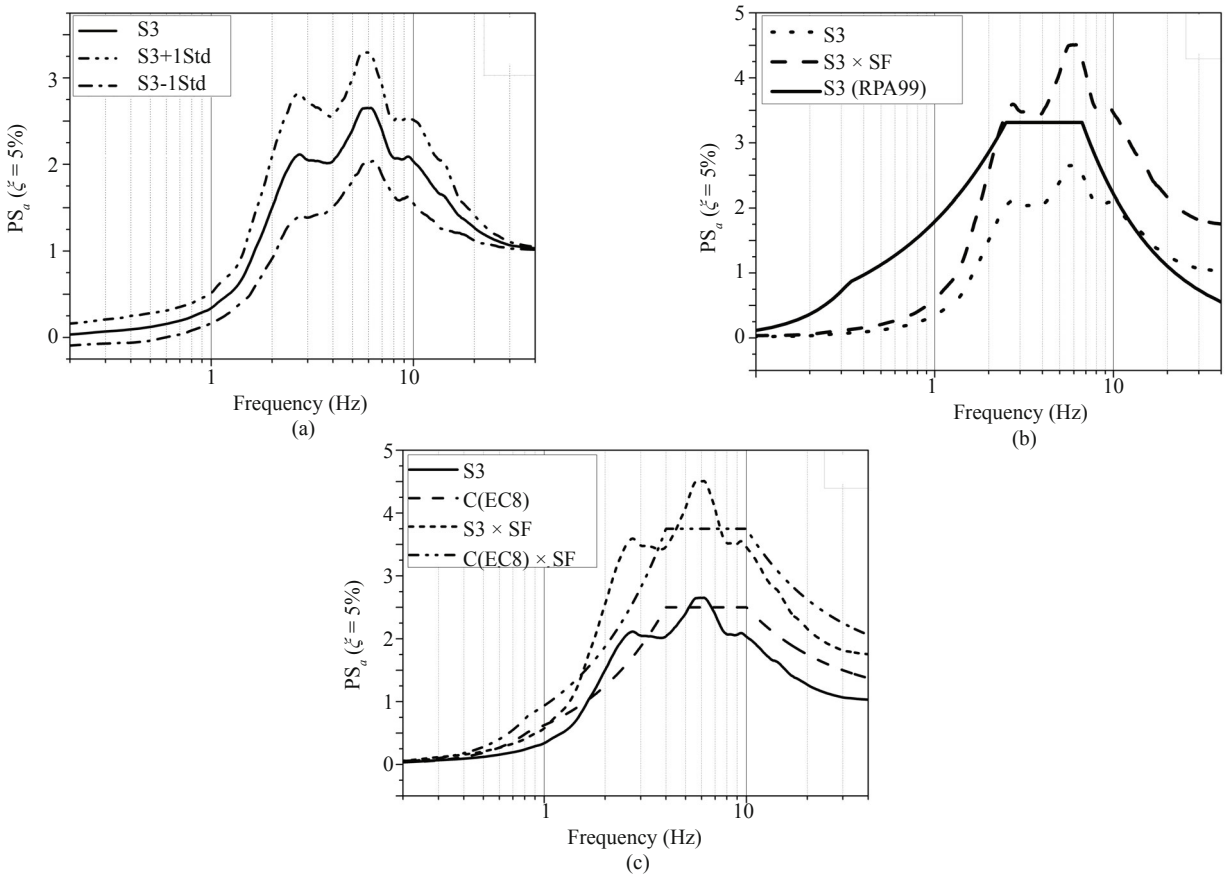

Fig. 12 Mean acceleration pseudo response spectrum with 5% damping of the S3 site. Normalized response spectrum is compared with the corresponding RPA99 S3 and EC8 C design response spectra

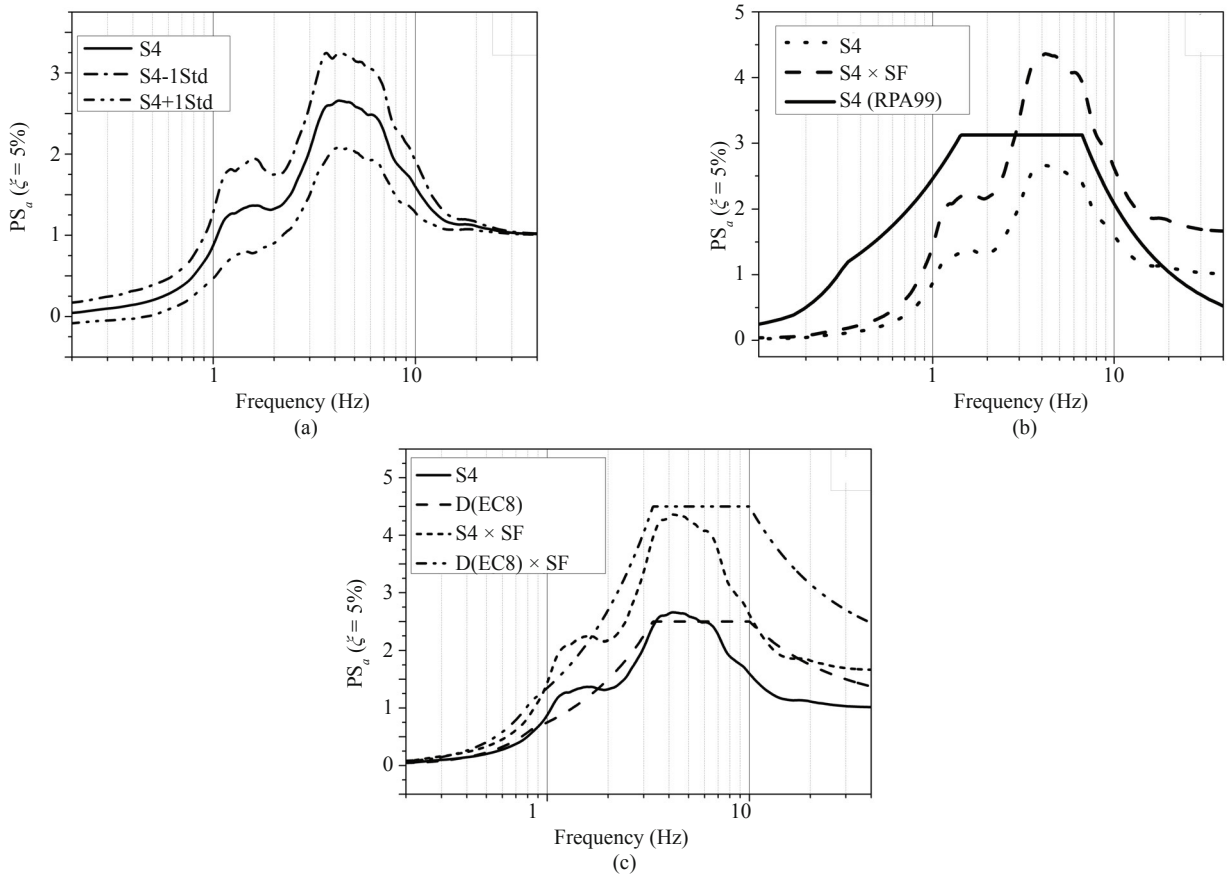

Fig. 13 Mean acceleration pseudo response spectrum with 5% damping of the S4 site. Normalized response spectrum is compared with the corresponding RPA99 S4 and EC8 D design response spectra before and after being combined with calculated site factorQ

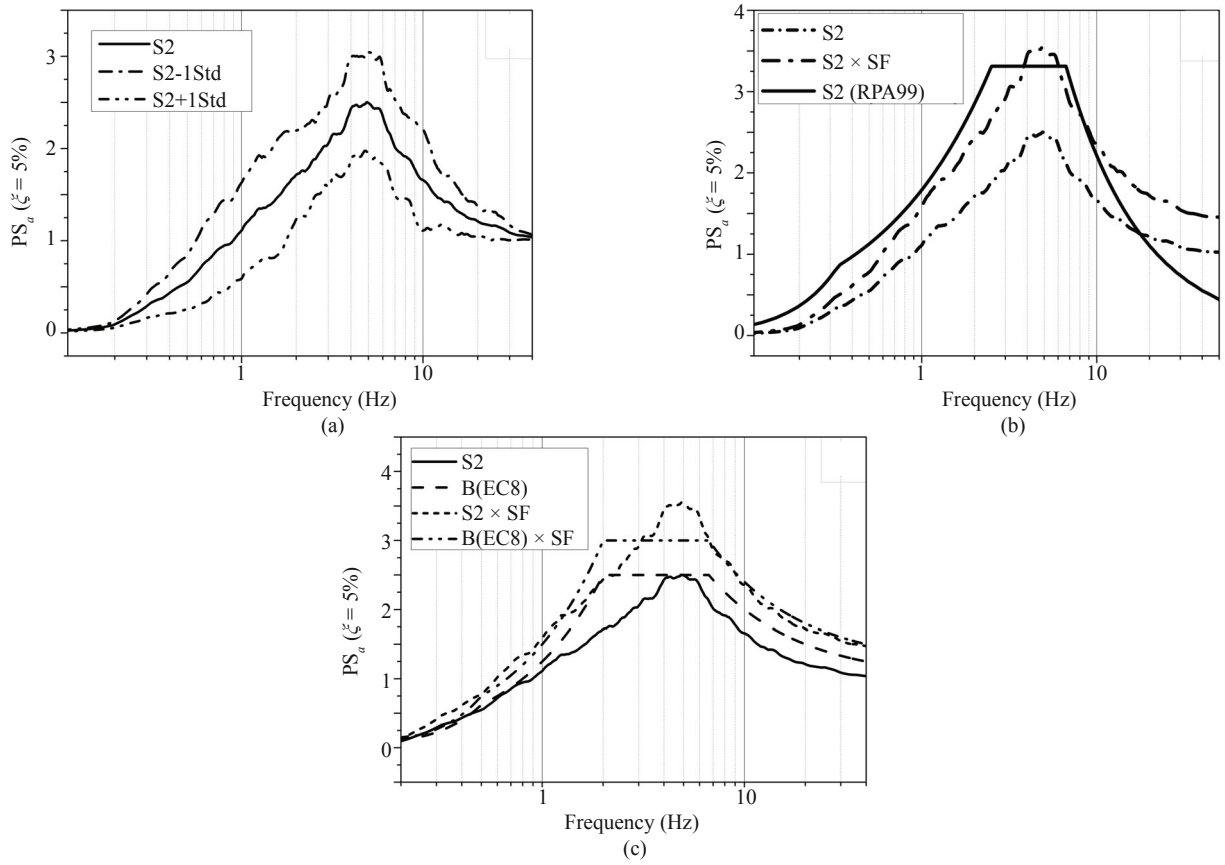

Fig. 14 Mean pseudo acceleration response spectrum with 5% damping of the S2 site. Normalized response spectrum is compared with the corresponding RPA99 S2 and EC8 B design response spectra before and after combining it with the corresponding mean site factor

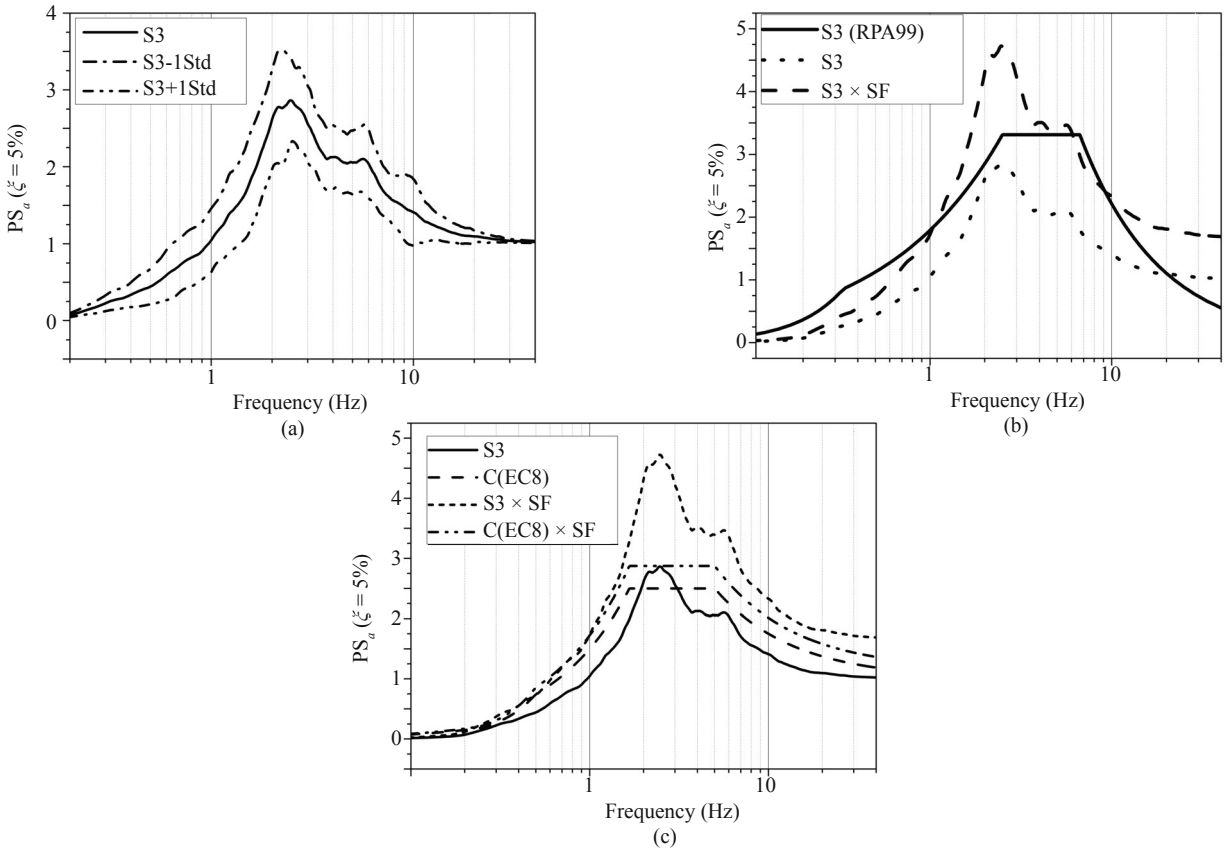

Fig. 15 Mean pseudo acceleration response spectrum with 5% damping of the S3 site. Normalized response spectrum is compared with the corresponding RPA99 S3 and EC8 C design response spectra before and after being combined with calculated site factor

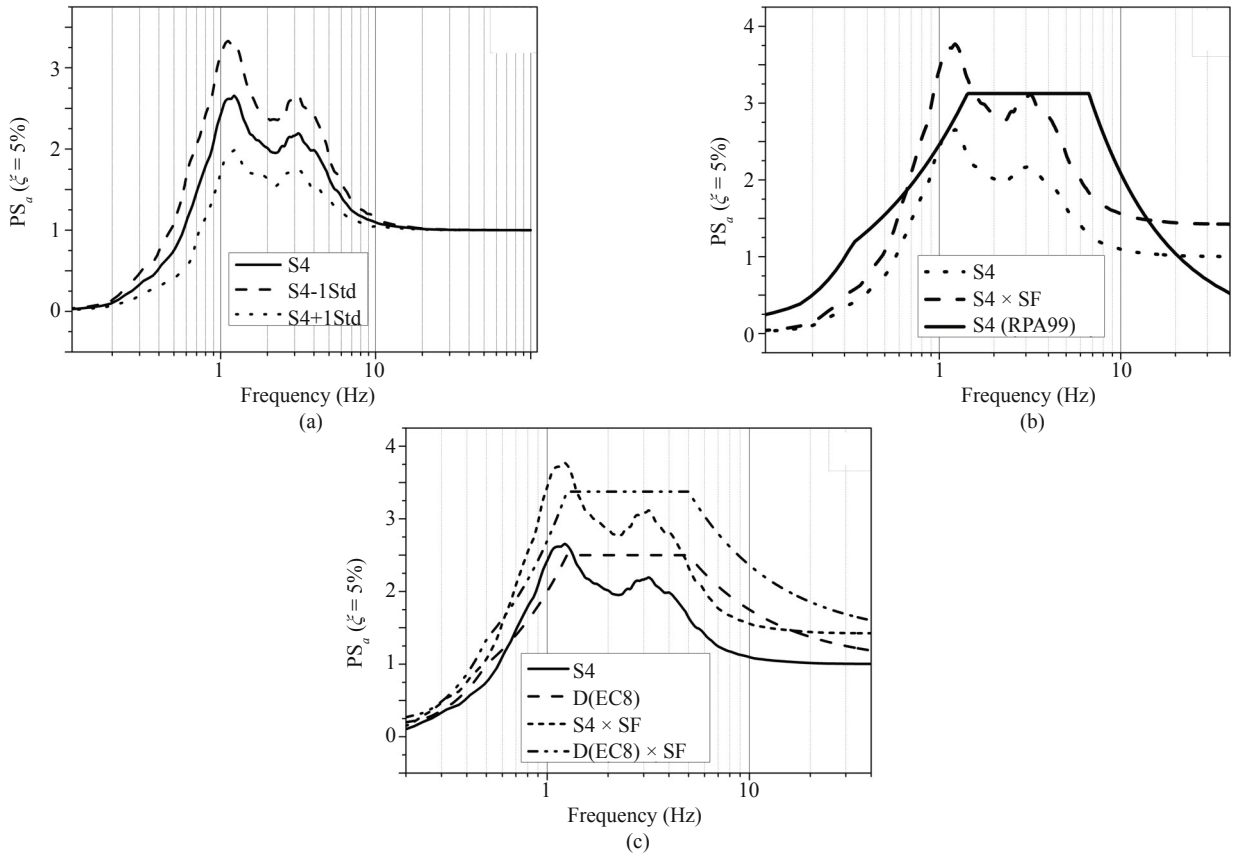

Fig. 16 Mean pseudo acceleration response spectrum with 5% damping of the S4 site. Normalized response spectrum is compared with the corresponding RPA99 S4 and EC8 D design response spectra before and after being combined with calculated site factor

design spectrum (Fig. 16(c)). The two curves match well in spectral amplitude up to 1.4 Hz; above 1.4 Hz, the calculated S4 spectral value is less than the EC8 D.

8 Conclusion

This study proposes a simple tool for RPA99 design site characterization, through average transfer functions via a probabilistic simulation approach combined to a statistical study. First step in the process is to simulate, for any RPA99 site type, many soil profile realizations that are consistent with the RPA99 requirements in terms of shear wave velocity interval. In the second step, deterministic calculations of the mean transfer functions via 1-D seismic analyses are made. The mean transfer function is a practical tool to characterize entire site objects of study and, henceforth, allows their classification by comparing the in-situ measured data with the proposed mean transfer functions. It is established that the frequency content of the transfer function is similar to the H/V amplification function. For the linear case, the mean transfer function curves show an important amplification level evidenced at frequencies greater than those of the equivalent linear case. The S2 mean transfer function curves are extremely close in both the linear and equivalent linear cases, with a common amplitude peak shown at practically the same frequency, an indication that nonlinear behaviour is minimal for this site type. S3 and S4 are, on the other hand, soft and very soft site, respectively, according to RPA99 provisions. Consequently, they exhibit nonlinearity effects characterized by a drop in maximal amplitude and a shift of the peak frequency shown through their corresponding transfer function curves.

The Kik-Net Japanese database is used to check the reliability of the transfer functions based classification scheme. A site classification test is made according to the RPA99 provisions. The obtained results indicate good classification of the soil profile when compared to the current Algerian seismic code classification. With the exception of one site, the mean transfer function (MTF) assigned classes within ±1 class were completely successful compared to the other classification. Classification is also made for station sites situated in the Mitidja basin (Algeria), where micro-tremor H/V spectral ratio curves were derived by Laouami and Slimani (2013). Comparison between H/V curves and the proposed transfer functions leads to a good classification of the Boumerdes, Dar el Beida, Hussein Dey and El Afroun stations.

Considering two acceleration records datasets (Type1 and Type 2 according to the current EC8), MTF is used to calculate the mean site factors and the normalized mean response spectra. The calculated mean site factors are of great interest since they represent a new dimension to site classification and ideal complement

to current RPA99 provisions, which do not integrate explicitly the site factor concept. The mean response spectra combined with mean site factors reveal important differences with the RPA99 design response spectra for almost all site classes. For the type 2 seismicity level, the mean response spectra shapes are not well matched with the RPA99 design response spectra, regarding both frequency range and spectral amplitudes, whereas they show good agreement with the corresponding EC8 design response spectra, with the exception of the S3 site which exhibits relatively larger spectral values than EC8 C. For the Type 1 seismicity level, the results show that unlike the other site classes, the S2 mean response spectrum shape is consistent with the corresponding RPA99 S2 design response spectrum for both frequency content and spectral amplitudes whereas the S3 and S4 plotted spectral shapes are, on average, in good agreement with those of EC8 when differences between their site factors are excluded. In particular, a large disparity is observed between the EC8 C and the S3 site factor values.

Calculated mean response spectra are realistic and more appropriate representation of a site because they are derived on rational basis and, more importantly, they embody the amplification potential of the site by virtue of the calculated mean transfer functions.

Acknowledgement

The authors would like to thank Mr. Abdenasser Slimani, Senior Researcher at the Earthquake Engineering Applied Research Center (CGS) and Mr. Mohamed Bendahgane, assistant professor at the civil engineering faculty of the USTHB, for their assistance and contribution. Several of their directions and suggestions have been adopted in this study.

References

Ambraseys N, Smit P, Sigbjornsson R, Suhadolc P and Margaris B (2002), *Internet-site for European Strong-Motion Data*. European Commission, Research-Directorate General, Environment and Climate Programme.

Ayadi A, Maouche S, Harbi A, MeghraouiM, Beldjoudi H, Oussadou F, Mahsas A, Benouar D, Heddar A, RouchicheY, Kherroubi A, Frogneux M, Lammali K, Benhamouda F,Sebai A, Bourouis S, Alasset PJ, Aoudia A, Cakir Z,Merahi M, Nouar, O, Yelles A, Bellik A, Briole P,Charade O, Thouvenot F, Semane F, Ferkoul A, Deramchi A and Haned SA (2003), "Strong Algerian Earthquake Strikes near Capital City," *EOS Trans. Am. Geophys. Union*, **84**: 561–568.

Bard PY (1999), "Microtremor Measurements: a Tool for Site Effect Estimation?" In: Irikura K, Kudo K, Okada H, Sasatani T (eds) *The Effects of Surface Geology on Seismic Motion*, Balkema, Rotterdam, pp 1251–1279.

Benouar D (1994), "The Seismicity of Algeria and Adjacent Regions," Annali Di Geofisica **37**: 459–862.

Borcherdt RD and Gibbs JF (1970), "Effect of Local Geological Conditions in the San Francisco Bay Region on Ground Motions and the Intensities of the 1906 Earthquake," *Bull. Seism. Soc. Am.*, **66**: 467–500.

Bouhadad Y and Laouami N (2002), "Earthquake Hazard Assessment in the Oran Region (Northwest Algeria)," *Natural Hazards*, **26**: 227–243.

Cadet H, Bard PY and Duval M (2008), "A New Proposal for Site Classification Based on Ambient Vibration Measurement and the Kik-net Strong Motion Data Set," *14th World Conference on Earthquake Engineering*, October 12-17, Beijing, China.

CRAAG (1994), "Les séismes de l'Algérie de 1365 à 1992," Publication du CRAAG, Alger, 227 p.

Eurocode 8 (2004), *Design of Structures for Earthquake Resistance*, *Part 1: General Rules, Seismic Actions and Rules for Buildings*, European Standard EN 1998-1:2004 Comité Européen de Normalisation, Brussels, Belgium,

Fenton AG and Griffiths DV (2000), "Bearing Capacity of Spatially Random Soils," *8th ASCE Conference on Probabilistic Mechanics and Structural Reliability*, PMC2000-097.

Ghasemi H, Zare M, Fukushima Y and Sinaeian F (2009), "Applying Empirical Method in Site Classification, Using Response Spectral Ratio (H/V), A Case Study on Iranian Strong Motion Network (ISMN)," *Soil Dynamics and Earthquake Engineering*, **29**: 121–132.

JICA and CGS (2006), "A Study of Seismic Microzoning of the Wilaya of Algiers in the People's Democratic Republic of Algeria," *Final Report*, **2**: Oyo International Corp. Nippon Koei Co., Ltd.

Kawase H, Sánchez-Sesma FJ and Matsushima S (2011), "The Optimal Use of Horizontal-to-vertical Spectral Ratios of Earthquake Motions for Velocity Inversions Based on Diffuse-field Theory for Plane Waves," *Bulletin of the Seismological Society of America*, **101**(5): 2001–2014.

Langston CA (1979), "Structure under Mount Rainier, Washington, Inferred from Teleseismic P and S Waves," *Journal of Geophysics Research*, **84**: 4749–4762.

Laouami N and Slimani A (2013), "Earthquake Induced Site Effect in the Algiers–Boumerdes Region: Relation between Spectral Ratios Higher Peaks and Observed Damage during the May 21st M_w 6.8 BoumerdesEarthquake (Algeria)," *Pure and Applied Geophysics*. DOI 10.1007/s00024-012-0612-3.

Laouami N, Slimani A, Bouhadad Y, Chatelain JL and Nour A (2006), "Evidence for Fault-related Directionality and Localized Site Effects from Strong Motion Recordings of the 2003 Boumerdes (Algeria) Earthquake: Consequences on Damage Distribution and the Algerian Seismic Code," *Soil Dynamics and*

Earthquake Engineering, **26**(11): 991–1003.

Lermo J and Chávez-García FJ (1993), "Site Effect Evaluation Using Spectral Aatios with Only One Station," *Bull Seismol Soc Am*, **83**: 1574–1594.

Lermo J and Chávez-García FJ (1994), "Site Effect Evaluation at Mexico City: Dominant Period and Relative Amplification from Strong Motion and Microtremor Records," *Soil Dynamics and Earthquake Engineering*, 13-6: 413-423.

Nakamura Y (1989), "A Method for Dynamic Characteristic Estimates of Subsurface Using Microtremor on the Ground Surface," *Q. Rep Railway Tech Res Inst*, **30**: 25–33.

Nogoshi M and Igarashi T (1971), "On the Amplitude Characteristics of Microtremor (Part 2) (in Japanese with English Abstract)," *Journal of Seismological Society of Japan*, **24**: 26-40.

Pitilakis K, Gazepis C and Anastasiadis A (2004), "Design Response Spectra and Soil Classification for Seismic Code Provisions," *Proceedings of 13th World Conference on Earthquake Engineering*, Paper n. 2904, Vancouver,B.C., Canada.

Pitilakis K, Riga E and Anastasiadis A (2012), "Design Spectra and Amplification Factors for Eurocode8," *Bull Earthquake Eng*, **10**: 1377-1400.

Pitilakis K, Riga E and Anastasiadis A (2012), "New Code Site Classification, Amplification Factors and Normalized Response Spectra Based on a World Wide Ground-motion Database," *Bull Earthquake Eng.*, **11**: 925–966.

Riepl J, Bard PY, Hatzfeld D, Papaioannou C and Nechtschein S (1998), "Detailed Evaluation of Site Response Estimation Methods across and along the Sedimentary Valley of Volvi (Euro-Seistest)," *Bull Seism Soc Am*, **88**: 488–502.

RPA99 (2003 Version), "Règles Parasismiques Algériennes., "D.T.R. –B.C. 2.48. National Center of Earthquake Applied Research (CGS), Rue Kaddour Rahim, BP 252, Hussein Dey, Algiers, Algeria. Imprimé par l'Office Nationale des Publications Universitaires (OPU). ISBN 9961-923-13-8.

Saman YS and Tsang HH (2011), "A New Site Classification Approach Based on Neural Networks," *Soil Dynamics and Earthquake Engineering*, **33**: 974–981.

Seed HB and Idriss IM (1970), "Soil Moduli and Damping Factors for Dynamic Response Analyses," Earthquake Engineering Research Center, *Report N°. EERC 70-10*, University of California, Berkeley, California.

Seed HB and Sun JH (1989), "Implication of Site Effects in the Mexico City Earthquake of September 19, 1985 for Earthquake-resistance-design Criteria in the San Francisco Bay Area of California," *Report N°. UCB/EERC-89/03*, University of California, Berkeley, California.

Seo K, Haile M, Kurita K, Yamazaki K and Nakamura A (1996), "Study of site effects in Kobe area using microtremors," *10th World Conference on Earthquake Engineering*, Acapulco, Mexico.

Wen R, Ren Y, Zhou Z and Shi D (2010), "Preliminary Site Classification of Free-field Strong Motion Stations Based on Wenchuan Earthquake Records," *Earthquake Science*, **23**: 101–110.

Zhao JX, Irikura K, Zhang J, Fukushima Y, Somerville PG, Asano A *et al*., (2006), "An Empirical Site-Classification Method for Strong Strong-motion Stations in Japan Using H/V response Spectral Ratio," *Bull Seismol Soc Am*, **96**(3): 914–925.

Zhao JX, Irikura K, Zhang J, Fukushima Y, Somerville PG and Saiki T (2004), "Site Classification for Strong Strong-motion Stations in Japan Using H/V Response Spectral Ratio," *Proceeding of 13th World Conference on Earthquake Engineering*, Vancouver, Canada.